pH SENSITIVE POLYMERIC NANOPARTICLES FABRICATED BY DISPERSION POLYMERIZATION FOR CANCER THERAPY

Emmanuel O. Akala
Department of Pharmaceutical Sciences, College of Pharmacy, Howard University, Washington DC, 20059

INTRODUCTION

•Administered bioactive agents distribute throughout the body, based on their physicochemical properties, before reaching the biophase or site of action resulting in side effects

•One way to address this problem is to formulate drug delivery systems such that they are capable of accumulating in desired pathological sites with little or no accumulation in non-target tissues[1]

•Recent studies on site-specific delivery of therapeutic and diagnostic agents have utilized environmental stimuli to trigger the release of the agents at a particular body compartment[1]

•Thus the use of stimuli-responsive nanocarriers offers an opportunity to make the delivery system become an active participant, rather than a passive vehicle, in the optimization of therapy

•Following cellular uptake via endocytosis, the nanocarrier system faces very well-defined compartments with strongly differential pH status. In cancer cells early endosome has a pH about 5–6 while the late lysosome, which is the most acidic compartment, has a pH around 4–5 . The extra- and intra-cellular pH gradients can be used to design drug delivery systems which selectively release the transported drug(s) at the biophase (specific site of delivery)[2]

METHODS AND RESULTS

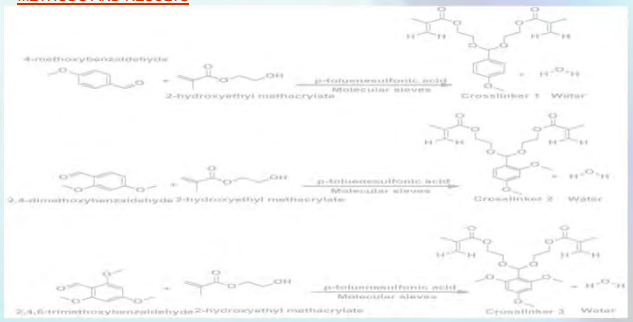

Figure1: Synthesis of Crosslinking Agents

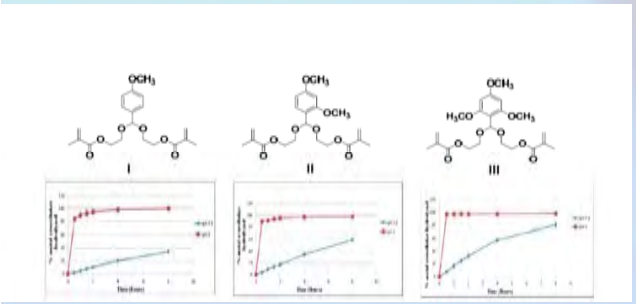

Figure 2: Efffects of Structure on the Hydrolysis of Benzaldehyde Bis-acrylate Acetal Crosslinkers at pH 5.0 and pH 7.4

Di (2-methacryloyloxyethoxy)-[4-methoxyphenyl]methane (Crosslinker I)
Di (2-methacryloyloxyethoxy)-[2, 4-dimethoxyphenyl]methane (Crosslinker II)
Di (2-methacryloyloxyethoxy)-[2, 4,6-trimethoxyphenyl]methane (Crosslinker III)

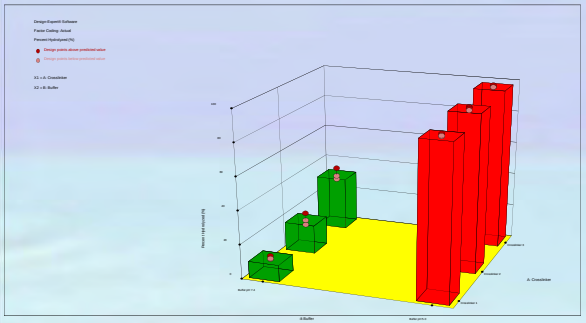

Figure 3: 3D Plot Showing the Effect of the Type of Crosslinker and Buffer on % of Crosslinker Hydrolyzed at 2 Hours.

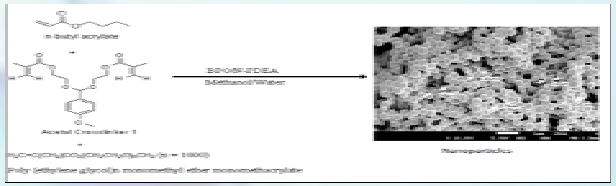

Figure 4: Synthesis of Nanoparticles by Dispersion Polymerization

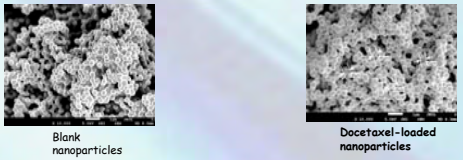

Figure 5: Scanning Electron Micrographs of Nanoparticles Fabricated with Crosslinker I [3,4]

Table 1: Average particle size, polydispersity index (PDi), zeta potential, encapsulation efficiency and loading efficiency of nanoparticles. (N = 3)[14]

Nanoparticle	Particle Size (nm)	PDI	Zeta Potential (mV)	Encapsulation efficiency (%)	Loading Efficiency (%)
Blank Nps_1	447.53 ± 7.53	0.21 ± 0.01	-45.27 ± 0.86	-	-
Dxtl-Nps_1	479.87 ± 5.12	0.14 ± 0.03	-47.33 ± 3.06	93.96 ± 0.25	0.45 ± 0.03
Blank Nps_2	205.87 ± 13.15	0.37 ± 0.05	-21.77 ± 1.33	-	-
Dxtl-Nps_2	265 ± 1.96	0.23 ± 0.003	-30.13 ± 0.51	90.48 ± 0.31	1.79 ± 0.24
Blank Nps_3	266.93 ± 2.71	0.22 ± 0.011	-36.27 ± 2.51	-	-
Dxtl-Nps_3	345.43 ± 7.09	0.38 ± 0.036	-41.07 ± 0.42	86.49 ± 1.46	1.08 ± 0.19

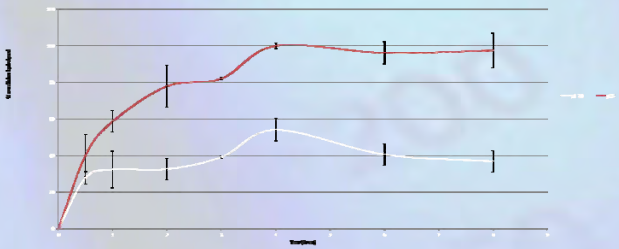

Figure 6: Hydrolysis studies of blank nanoparticles fabricated with crosslinker I. Similar data were obtained with crosslinkers II and III

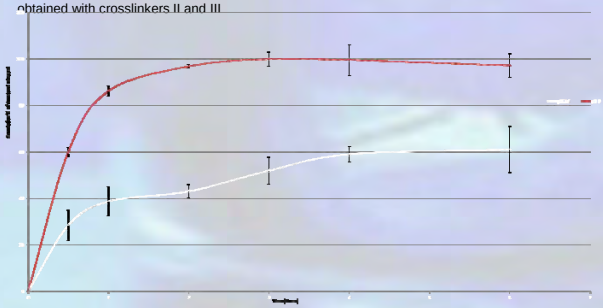

Figure 7: Drug release curves of docetaxel-loaded nanoparticles fabricated with crosslinker III at pH 7.4 and pH 5.0 (N = 3) [5]. Similar data were obtained with crosslinkers I and II

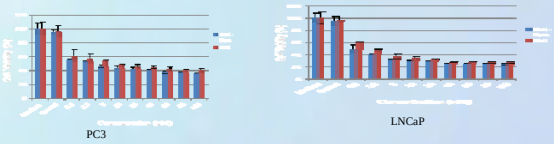

Figure 8: Comparison of the effect of docetaxel-loaded nanoparticles (Dxtl-nps) and docetaxel solution (Dxtl) on the cell viability ff PC3 And LNCAP cells Post 72 hours Of treatment

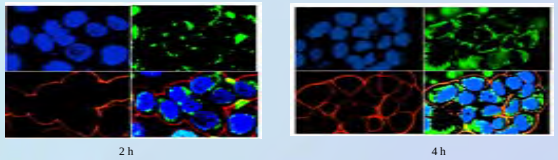

Figure 9: Cell internalization studies of MCF-7 cells with Rhodamine-123 loaded nanoparticles. Similar results were obtained with PC3 cells

Cellular uptake images of MCF-7 cells after 2 hours and 4 hours of incubation with 250 µg /ml of rhodamine-123 loaded nanoparticles. Upper left quadrant shows nuclei stained blue with Hoechst® 33342 dye; lower left quadrant shows cell membrane stained red with CellMaskTM deep orange plasma membrane stain; upper right quadrant shows green stained rhodamine-123 loaded nanoparticles and lower right quadrant shows overlay of all the three quadrants. [2,6]

CONCLUSION

- Three pH-sensitive acetal crosslinkers were synthesized and characterized
- Spherical and fairly monodispersed nanoparticles were formed by dispersion polymerization technique
- Hydrolysis studies and drug release studies confirmed pH-
- The pH-sensitive nanoparticles degraded quickly in the mildly acidic environments similar to those found in endosomes and lysosomes of tumor tissues.
- In vitro cell viability assay showed that the docetaxel-loaded nanoparticles were as effective as free drug in causing cell death in both PC3 and LNCaP cell lines.
- These novel pH-sensitive nanoparticles would offer several advantages over conventional drug therapies

REFERENCES

1. Puri R, Berhe SA, Akala EO. pH-sensitive polymeric nanoparticles fabricated by dispersion polymerization for the delivery of bioactive agents. Pharma Nanotech. 2017;5:1-28
2. Reema Puri, Simeon Adesina, Emmanuel Akala. Cellular uptake and cytotoxicity studies of pH-responsive polymeric nanoparticles fabricated by dispersion polymerization J Nanosci Nanomed. Vol.2 No.1 April-2018., 1-18
3. Ogunwuyi O, Adesina S, Akala EO. D-Optimal mixture experimental design for stealth biodegradable crosslinked docetaxelloaded poly-caprolactone nanoparticles manufactured by dispersion polymerization. Pharmazie 2015;70:165-76.
4. Adesina SK, Wight SA, Akala EO. Optimization of the fabrication of novel stealth PLA based nanoparticles by dispersion polymerization using D-optimal mixture design. Drug Dev Ind Pharm.2014;40:1547-56.
5. Akala EO, Okunola O. Novel stealth degradable nanoparticles prepared by dispersion polymerization for the delivery of bioactive agents. Part I. Pharm Ind. 2013;75:
6. Adesina SK, Holly A, Kramer-Marek G, Capal J, and Akala EO. Polylactide-based Paclitaxel-loaded Nanoparticles Fabricated by Dispersion Polymerization: Characterization, Evaluation in Cancer Cell Lines, and Preliminary Biodistribution Studies. J Pharma Sci. 2014;103:2546-55.

ACKNOWLEDGEMENTS

This work was supported in part by NCI/NIH Grant #: 1SC2CA138179-01 and NCI/NIH Grant 1SC1CA199810-01
This work was carried out in facilities supported by NCRR/NIH Grants #1 C06 RR 020608-01 a #1 C06 RR 14469-01.